Changes in tear film pH alter the rate of ocular penetration of topically applied drugs that are weak acids or bases, because the ratio of their ionized to unionized form is a function of pH and because ionized molecules do not easily penetrate the cornea. Pilocarpine, a case in point, is a weak base, pKa 7.07, but is formulated as a salt in eyedrop preparations. Pilocarpine nitrate at 0.1 *M* in water at 20° has an equilibrium pH of 3.9, but the pH of pilocarpine nitrate ophthalmic formulations is adjusted to 4–5. Altering the pH of tears toward the acid side increases the proportion of protonated pilocarpine to the unionized pilocarpine base in the tears, and the rate of penetration of the drug to the internal eye is expected to decrease.

Anderson and Cowles (4) showed that pilocarpine is a more effective ocular hypotensive agent when administered at pH 6.5 (22% unionized) than at pH 5 (1% unionized). They suggested that this enhanced efficacy at pH 6.5 is a result of increased penetration of pilocarpine due to a greater concentration of the unionized form of the drug. These results suggest that, for a given pilocarpine concentration, more drug will enter the eye if the physiological pH of the tear film can be maintained coincident with drug administration. Unfortunately, the pH of eyedrop solutions must be kept low at present to stabilize the pilocarpine, necessitating larger doses for therapeutic effect than would otherwise be required with more nearly physiological pH.

Fairbairn *et al.* (5) indicated that a more concentrated acid buffer causes a stronger sensation of stinging or burning than does a less concentrated buffer of the same acid pH. Presumably, this sensory effect occurs because the tear film remains at a lower pH for a longer time with the more concentrated buffer. Fairbairn *et al.* (5) recommended minimum buffering of acidic ophthalmic solutions to permit the tear film to return to the physiological pH range rapidly. This conclusion, that the stronger the acid buffer the more subjectively irritating the eyedrop, appears valid for pilocarpine solutions.

Pilocarpine exerts no known topical anesthetic effect, so it should not suppress any stinging sensation caused by a lowering of eye surface pH. The combination of drug and excipients causes at least as great a sensation of burning and stinging as a solution of pharmacologically inactive salt with identical buffer capacity. Whether or not pilocarpine solutions are subjectively more irritating at lower pH values depends not only on the extent and duration of the induced pH change but also on the relative potential for irritation of the protonated *versus* the base form of drug. This question awaits further investigation.

Hydrochloric acid alone in pH 4 solutions produced smaller decreases in tear film pH, and the recovery time to pretreatment tear film pH was shorter by 15 min than with any 2% pilocarpine solution tested. Attempts to prolong residence time of pilocarpine in the eye by adding macromolecules to the formulation (Solution D) appeared to prolong the duration of pH change as well.

The results of this study indicate that reduction of tear film pH by pilocarpine eyedrop formulations is not a simple function of solution pH. On the contrary, both the contact time and the acidic buffer capacity of these solutions contribute to the magnitude and duration of lowered tear film pH after an eyedrop of an ophthalmic pilocarpine formulation is instilled.

The continuous delivery of pilocarpine base in the absence of concomitant delivery of acid buffers favors the prevalence of the neutral base form of pilocarpine. The neutral form of pilocarpine should readily penetrate the lipophilic corneal epithelial barrier, in contrast to the protonated form which predominates at pH < 7. This reasoning may partially explain why continuous delivery of pilocarpine is clinically effective at daily doses of one-fourth to one-eighth (6, 7), and occasionally as little as one-fourteenth (8), those usually administered by eyedrops.

REFERENCES

(1) S. S. Chrai, T. Patton, A. Mehta, and J. Robinson, *J. Pharm. Sci.*, **62**, 1112(1973).

(2) N. Keller, D. M. Moore, and J. Urquhart, "Pilocarpine Kinetics in Rabbit Eye Tear Film during Continuous Administration," presented at ARVO meeting, Sarasota, Fla., Apr. 28, 1976.

(3) R. A. Moses, "Adler's Physiology of the Eye," 5th ed., Mosby, St. Louis, Mo., 1970, p. 21.

(4) R. A. Anderson and J. B. Cowles, *Br. J. Ophthalmol.*, **52**, 607(1968).

(5) W. Fairbairn, W. Shepherd, and S. Eriksen, in preparation, cited by Allergan Pharmaceuticals, *J. Am. Optom. Assoc.*, **40**, 720(1969).

(6) P. Lee, Y. Shen, and M. Eberle, *Invest. Ophthalmol.*, **14**, 43(1975).

(7) M. S. Armaly and K. R. Rao, in "Symposium on Ocular Therapy," I. H. Leopold, Ed., Mosby, St. Louis, Mo., 1973, pp. 80–94.

(8) K. L. Macoul and D. Pavan-Langston, *Arch. Ophthalmol.*, **93**, 587(1975).

ACKNOWLEDGMENTS AND ADDRESSES

Received October 15, 1975, from *Alza Research, a Division of Alza Corporation, Palo Alto, CA 94304*

Accepted for publication February 9, 1976.

[x] To whom inquiries should be directed.

Bioavailability Assessment under Quasi- and Nonsteady-State Conditions III: Application

J. V. BONDI, H. B. HUCKER, K. C. YEH, and K. C. KWAN [x]

Abstract □ The applicability of bioavailability assessment at quasi- and nonsteady state is illustrated with data from a study comparing two formulations of amitriptyline hydrochloride in humans. Relative bioavailability as a function of the observed mean plasma concentrations may be expressed in closed form, provided the affected intervals begin and end in the log–linear region. Alternatively, numerical, graphical, and/or electronic computational techniques may be used to simulate the appropriate $[\overline{C}p^{(i)}]_{sim}$, the proximity of which to $[\overline{C}p^{(i)}]_{obs}$ is a function of relative bioavailability and of ω. If a model can be found to fit the data adequately, it would be sufficient that only one sampled interval end in the log–linear phase.

Keyphrases □ Bioavailability—amitriptyline hydrochloride, assessment at quasi- and nonsteady state, equations derived □ Amitriptyline hydrochloride—bioavailability assessment at quasi- and nonsteady state, equations derived □ Antidepressants—amitriptyline hydrochloride, bioavailability assessment at quasi- and nonsteady state, equations derived

Previous reports (1, 2) in this series dealt with the theoretical basis for bioavailability assessment at quasi- and nonsteady state and its versatility in accommodating variations in experimental design. The purpose of this report is to apply the proposed technique to data from a study comparing two different formulations of

amitriptyline hydrochloride in humans. Details of the study design and of the results were given elsewhere (3); only elements pertinent to the present discussion are repeated here. This example was chosen because several aspects in its design permit considerations of alternative means of estimating relative bioavailability from a given set of results.

The possible analytical options considered include those that attempt to make projections concerning the steady state, those that attempt the opposite of extrapolating to time zero, and some combinations of the two. It is shown that the various approaches are equivalent and that similar conclusions result from these divergent lines of reasoning. Since the various ramifications of the method cannot be exhaustively treated with a single example, other approaches that may have been possible are also discussed.

EXPERIMENTAL

The study was conducted with 12 healthy volunteers over 2 weeks. In Period I (Days 1–7), each subject ingested one 25-mg amitriptyline hydrochloride tablet at 8 am, 2 pm, and 8 pm daily. During Period II (Days 8–14), the same subjects ingested one 75-mg amitriptyline hydrochloride capsule at 8 am daily. On Days 7 and 14, plasma samples were drawn at 8, 9, 10, and 11 am, 12 noon, 2, 5, and 8 pm, and 8 am of the following day. Plasma amitriptyline concentrations were determined by the method of Hucker and Stauffer (4).

DRUG ACCUMULATION

Closed-Form Solutions (Method A)—Since the daily dosage is the same between treatments, the simplest approach would have been to compare individual mean steady-state plasma concentrations, $\overline{C}p^{(ss)}$, projected from the observed mean plasma levels on Day 7, $\overline{C}p^{(7)}$, and on Day 14, $\overline{C}p^{(7+7)}$. The mean plasma concentration on Day 7 is the weighted sum of the mean plasma levels $\overline{C}p^{(7,\tau_1)}$, $\overline{C}p^{(7,\tau_2)}$, and $\overline{C}p^{(7,\tau_3)}$ over each of the three dosing intervals τ_1, τ_2, and τ_3; *i.e.*:

$$\overline{C}p^{(7)} = \frac{\tau_1\overline{C}p^{(7,\tau_1)} + \tau_2\overline{C}p^{(7,\tau_2)} + \tau_3\overline{C}p^{(7,\tau_3)}}{\tau_1 + \tau_2 + \tau_3} \qquad \text{(Eq. 1)}$$

since $\tau_1 + \tau_2 + \tau_3 = 24$ hr, the mean daily plasma concentration at steady state for the prescribed tablet dosage regimen is:

$$[\overline{C}p^{(ss)}]_T = \frac{\overline{C}p^{(7)}}{1 - e^{-7\omega(\tau_1+\tau_2+\tau_3)}} \qquad \text{(Eq. 2)}$$

where ω is the observed terminal slope. Similarly, the mean plasma level over a 24-hr interval at steady state following daily administrations of the capsule formulation is given by:

$$[\overline{C}p^{(ss)}]_C = \frac{\overline{C}p^{(7+7)} - \overline{C}p^{(7)}e^{-7\omega\phi}}{1 - e^{-7\omega\phi}} \qquad \text{(Eq. 3)}$$

where ϕ is the dosing interval for capsules, and the subscripts T and C refer to tablets and capsules, respectively. The numerator of Eq. 3 is the expected mean plasma level after seven daily doses of the capsule formulation represented as the difference between the observed mean on Day 14 and the residual contributions resulting from the prior administration of tablets for 7 days.

The relative bioavailability between the tablet and capsule formulations, F_C/F_T, can be estimated by the ratio of their mean plasma levels at steady state. Combining Eqs. 2 and 3 and rearranging give:

$$\frac{F_C}{F_T} = \frac{\overline{C}p^{(7+7)}}{\overline{C}p^{(7)}} - e^{-7\omega\phi} \qquad \text{(Eq. 4)}$$

Unfortunately, the sampling schedule does not permit satisfactory estimates of $\overline{C}p^{(7,\tau_2)}$ and $\overline{C}p^{(7,\tau_3)}$. Thus, prudence dictates that the analysis should be based on $\overline{C}p^{(7,\tau_1)}$ and $\overline{C}p^{(14,\phi)}$, mean plasma levels during τ_1 on Day 7 and during ϕ on Day 14, respectively. This type of study design is similar to previously described types (2). However, an extension of the general solutions (2) is necessary to account for the intervention of two additional tablet doses between the sampled interval of Period I and the beginning of Period II. In the prevailing situation of r daily doses of tablets for L days in Period I followed by u daily doses of capsules for M days in Period II, it can be shown that the appropriate solution is:

$$\left(\frac{F_{II}}{F_I}\right)_{T/C} = \frac{D_I}{D_{II}}\left\{\frac{[R_I]}{[R_{II}]}\frac{\overline{C}p^{(II,\phi)}}{\overline{C}p^{(I,\tau_1)}}\frac{\phi(1 - e^{-\omega\tau_1})}{\tau_1(1 - e^{-\omega\phi})} - \frac{[R_I']}{[R_{II}]}W\right\} \qquad \text{(Eq. 5)}$$

where D is the dose, $[R_i]$'s are the regimen factors, W is the residue factor, I is identified with tablets in Period I, and II is identified with capsules in Period II. In particular, when $r = 3$, $u = 1$, $l = 3$, $\tau_1 = \tau_2 = 6$ hr, $\tau_3 = 12$ hr, and $\overline{C}p^{(I,\tau_1)}$ is estimated on the Kth ($K \leq L$) day of Period I:

$$[R_I] = (e^{-24\omega})\sum_{j=1}^{r}\left(\prod_{i=1}^{j} e^{\omega\tau_i}\right) - (e^{-24K\omega})\left[1 + \sum_{j=1}^{r-1}\left(\prod_{i=1}^{j} e^{\omega\tau_i}\right)\right] \qquad \text{(Eq. 6a)}$$

$$[R_I] = 1 + e^{-12\omega} + e^{-18\omega} - e^{-24K\omega}(1 + e^{6\omega} + e^{12\omega}) \qquad \text{(Eq. 6b)}$$

$$[R_I'] = (e^{\omega\tau_l})\sum_{j=1}^{l}\left(\prod_{i=j}^{l} e^{-\omega\tau_i}\right) + (e^{-24\omega})\sum_{j=l}^{r-1}\left(\prod_{i=l}^{j} e^{\omega\tau_i}\right) - (e^{-24L\omega})\left(\prod_{i=1}^{l-1} e^{-\omega\tau_i}\right)\left[1 + \sum_{j=1}^{r-1}\left(\prod_{i=1}^{j} e^{\omega\tau_i}\right)\right] \qquad \text{(Eq. 7a)}$$

$$[R_I'] = (1 - e^{-24L\omega})(1 + e^{-6\omega} + e^{-12\omega}) \qquad \text{(Eq. 7b)}$$

$$[R_{II}] = (e^{-24\omega})\sum_{j=1}^{u}\left(\prod_{i=1}^{j} e^{\omega\phi_i}\right) - (e^{-24M\omega})\left[1 + \sum_{j=1}^{u-1}\left(\prod_{i=1}^{j} e^{\omega\phi_i}\right)\right] \qquad \text{(Eq. 8a)}$$

$$[R_{II}] = 1 - e^{-24M\omega} \qquad \text{(Eq. 8b)}$$

and:

$$W = \left(\prod_{i=l}^{r} e^{-\omega\tau_i}\right) e^{-24(M-1)\omega} = (e^{-12\omega})e^{-24(M-1)\omega} \qquad \text{(Eq. 9)}$$

For the present study, $K = L = M = 7$ days such that $\overline{C}p^{(I,\tau_1)}$ is synonymous with $\overline{C}p^{(7,\tau_1)}$ and $\overline{C}p^{(II,\phi)}$ is synonymous with $\overline{C}p^{(14,\phi)}$. However, for the time being, the general notation is retained to facilitate discussion. Whereas the regimen factors, $[R_i]$, serve the same functions previously ascribed (2), their specific combinations in this case should be noted. The inequality between $[R_I]$ and $[R_I']$ is caused by the two additional tablet dosages on Day 7. The ratio $[R_I]/[R_{II}]$ tracks the dosage intervals over which mean plasma levels are determined; the ratio $[R_I']/[R_{II}]$ accounts for the fact that the washout period begins two doses after the one for which estimates of mean plasma concentrations are made in Period I. In other words, the mean plasma concentration ratio and the residue factor share a common regimen factor only when the sampled interval and the washout period begin at the same time.

Simulations (Methods B and C)—Even though relative bioavailability ratios for any tractable dosing sequence would be amenable to solution in closed form, their complexity multiplies rapidly with each additional variant in dosage and dosage regimen and may become a deterrent in general usage. For this reason and for completeness, a somewhat more circuitous approach is suggested that may be of practical utility in some instances.

The strategy evolves with some initial assumptions concerning the ratio of F_C to F_T, which results in the observed plasma concentrations on Day 14. From the observed terminal slope ω and the mean plasma level $\overline{C}p^{(14,\phi)}$, the entire time course of change in plasma concentrations from time zero can be reconstructed through simulation. The validity of the initial assumptions will be reflected in the agreement, or the lack thereof, between simulated and observed plasma levels on Day 7. It will be shown that the ratio of simulated to observed mean plasma levels is a function of the relative bioavailability between treatments I and II. Alternatively, the bioavailability ratio can be varied iteratively until there is agreement between simulated and observed values.

For the prescribed dosing sequence, the mean plasma concentration during any capsule dosage interval in Period II can be represented by:

$$\overline{C}p^{(II,\phi)} = \frac{(1 - e^{-\omega\phi})}{\omega\phi V_0(1 - e^{-24\omega})}\{F_T D_T[R_I']W + F_C D_C[R_{II}]\} \qquad \text{(Eq. 10)}$$

where V_0 is as defined previously (1).

If Period II is prolonged indefinitely (*i.e.*, $M \to \infty$), a steady state for the capsule dosage regimen is attained. When $L = 7$ days and ϕ

= 24 hr:

$$[\overline{C}p^{(II,\phi)}] \lim_{M \to \infty} = [\overline{C}p^{(ss)}]_C = \frac{F_C D_C}{\omega \phi V_0} \quad \text{(Eq. 11)}$$

By substituting Eq. 11 into Eq. 10 and specifying $M = 7$:

$$\overline{C}p^{(14,\phi)} = [\overline{C}p^{(ss)}]_C \left\{ \frac{F_T D_T}{F_C D_C} [R_I'] W + [R_{II}] \right\} \quad \text{(Eq. 12)}$$

Initially, it is assumed that $F_C = F_T$. Under this assumption, $[\overline{C}p^{(ss)}]_C$ can be calculated from $[\overline{C}p^{(14,\phi)}]_{obs}$, the observed mean plasma level on Day 14; *i.e.*:

$$[\overline{C}p^{(ss)}]_C = \frac{D_C [\overline{C}p^{(14,\phi)}]_{obs}}{D_T [R_I'] W + D_C [R_{II}]} = \frac{F_C D_C}{\omega \phi V_0} \quad \text{(Eq. 13)}$$

and:

$$\frac{F_C}{V_0} = \frac{\omega \phi [\overline{C}p^{(14,\phi)}]_{obs}}{D_T [R_I'] W + D_C [R_{II}]} \quad \text{(Eq. 14)}$$

Next, it is assumed also that drug disposition kinetics obey a one-compartment open model with first-order absorption, for which the time course of change of Cp following a single dose of the tablet is given by the familiar:

$$Cp(t) = \frac{k_a F_T D_T}{(k_a - \omega) V_0} (e^{-\omega t} - e^{-k_a t}) \quad \text{(Eq. 15)}$$

In a one-compartment open model, $V_0 = V_d$, the apparent volume of distribution. The entire time course of drug accumulation during Period I according to the actual dosage schedule can now be simulated by appropriate summations of Eq. 15 over all dosing intervals, preferably with the aid of analog (5) or digital (6) computational techniques. Given the assumption of $F_C = F_T$, the only indeterminate quantity on the right-hand side of Eq. 15 is k_a, which can be chosen to reflect best the shape of the data on Day 7, with particular emphasis given to the morning dose.

From the simulated data, the mean plasma levels over τ_1 on Day 7, $[\overline{C}p^{(7,\tau_1)}]_{sim}$, can be calculated and compared with those observed, $[\overline{C}p^{(7,\tau_1)}]_{obs}$. Perfect agreement between observed and simulated data affirms the initial assumption of $F_C = F_T$. In any event, the ratio of simulated to observed data is a measure of F_C/F_T. For the prescribed tablet regimen, the general relationship between F_C/F_T and $[\overline{C}p^{(K,\tau_1)}]_{sim}/[\overline{C}p^{(K,\tau_1)}]_{obs}$ can be represented by:

$$\frac{F_C}{F_T} = \left\{ 1 + \frac{D_T}{D_C} \frac{[R_I']}{[R_{II}]} W \right\} \frac{[\overline{C}p^{(K,\tau_1)}]_{sim}}{[\overline{C}p^{(K,\tau_1)}]_{obs}} - \frac{D_T}{D_C} \frac{[R_I']}{[R_{II}]} W \quad \text{(Eq. 16)}$$

which is the equation of a straight line whose slope and intercept are functions of D, L, M, and ω. A diagrammatic representation of this relationship as a function of ω for the prevailing conditions of $D_T/D_C = 1/3$ and $L = M = 7$ is shown in Fig. 1. It is apparent that plots of F_C/F_T *versus* $[\overline{C}p^{(K,\tau_1)}]_{sim}/[\overline{C}p^{(K,\tau_1)}]_{obs}$ result in a family of straight lines, each passing through the point (1,1) with a different slope. The slopes vary inversely with ω. The lines converge to a limiting slope of unity (and, therefore, an intercept of zero) as ω becomes large.

In other words, with a given dosage regimen, steady state can be achieved sooner with drugs having shorter half-lives; at steady state, there is a one-to-one correspondence between the ratio $[\overline{C}p^{(K,\tau_1)}]_{sim}/[\overline{C}p^{(K,\tau_1)}]_{obs}$ and relative bioavailability. The regimen factor $[R_I]$ does not appear in Eq. 16, because the relationship between F_C/F_T and $[\overline{C}p^{(K,\tau_1)}]_{sim}/[\overline{C}p^{(K,\tau_1)}]_{obs}$ is independent of the location of the sampled interval in Period I.

In the present example, the specific comparison is between $[\overline{C}p^{(7,\tau_1)}]_{sim}$ and $[\overline{C}p^{(7,\tau_1)}]_{obs}$. Estimates of relative bioavailability can be obtained by setting $L = M = 7$ in Eq. 16 or by interpolating directly from Fig. 1 (Method B). Alternatively, F_C/F_T can be varied iteratively through repeated simulations such that equality between $[\overline{C}p^{(7,\tau_1)}]_{sim}$ and $[\overline{C}p^{(7,\tau_1)}]_{obs}$ and between $[\overline{C}p^{(14,\phi)}]_{sim}$ and $[\overline{C}p^{(14,\phi)}]_{obs}$ is achieved simultaneously after k_a has been fixed by the shape of the observed plasma concentration profile on Day 7 (Method C).

RESULTS

The mean plasma amitriptyline concentrations following the first tablet dosage on Day 7, $\overline{C}p^{(7,\tau_1)}$, and following the capsule dosage on Day 14, $\overline{C}p^{(14,\phi)}$ were estimated by:

$$\overline{C}p^{(7,\tau_1)} = \frac{\int_0^{\tau_1} Cp(t')dt'}{\tau_1} \quad \text{(Eq. 17)}$$

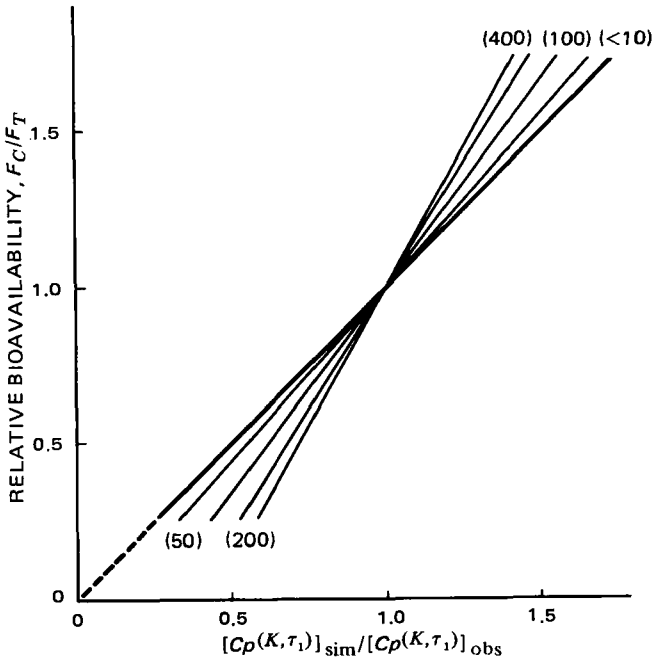

Figure 1—*Graphical representation of Eq. 16 for the prescribed dosing regimen. Values in parentheses correspond to plasma half-lives in hours.*

and:

$$\overline{C}p^{(14,\phi)} = \frac{\int_0^{\phi} Cp(t')dt'}{\phi} \quad \text{(Eq. 18)}$$

where τ_1 and ϕ equal 6 and 24 hr, respectively; t' is time from the last dose; and the areas under the plasma–time curve are trapezoidal approximations. Terminal slopes, ω, were estimated from the last data points on Day 14. Apparent lag times, t_0', and peak times, t'_{max}, for the sampled interval τ_1 on Day 7 were estimated visually from graphs of plasma concentration *versus* time. Individual values for $\overline{C}p^{(7,\tau_1)}$, $\overline{C}p^{(14,\phi)}$, t_0', t'_{max}, ω, and plasma half-life ($0.693/\omega$) are shown in Table I.

Method A—Estimates of relative bioavailability between the tablet and capsule formulations calculated by Eq. 5 are shown in Table II, which also includes the corresponding dosage, regimen, correction, and residue factors. Since the residue factor W is zero at steady state, its relatively minor contributions signify the fact that steady state is being approached in nearly every case. That is, given the observed terminal slopes, the plasma levels attained after 7 days of either treatment are very nearly those expected at steady state. On the other hand, the proximity between $\overline{C}p^{(14,\phi)}/\overline{C}p^{(7,\tau_1)}$ and F_C/F_T is purely coincidental since, in general, $[\overline{C}p^{(II,\phi)}]/[\overline{C}p^{(I,\tau_1)}]$ does not equal F_{II}/F_I at steady state.

Method B—Alternatively, estimates of relative bioavailability can be made from data presented in Table I under the initial assumption

Table I—Summary of Experimentally Observed Variables

Subject	Day 7 $\overline{C}p^{(7,\tau_1)}$, ng/ml	Day 7 t_0', hr	Day 7 t'_{max}, hr	Day 14 $\overline{C}p^{(14,\phi)}$, ng/ml	Day 14 ω, hr^{-1}	Day 14 $0.693/\omega$, hr
1	38.5	2	3	43.5	0.0133	52
2	65.4	0	1	74.5	0.0182	38
3	82.6	0	2	75.5	0.0204	34
4	71.3	1	4	72.3	0.0330	21
5	52.0	1	2	52.8	0.0433	16
6	22.8	2	6	39.5	0.0144	48
7	66.8	2	4	56.2	0.0347	20
8	52.9	2	6	68.4	0.0178	39
9	30.8	1	4	22.5	0.0231	30
10	60.2	1	3	79.2	0.0173	31
11	38.3	1	4	55.1	0.0217	32
12	64.3	0	1	52.1	0.0267	26

Table II—Estimates of Bioavailability by Projections to Steady State[a] (Eq. 5)

Subject	Mean Plasma Ratio, $\bar{C}p^{(II,\phi)}/\bar{C}p^{(I,\tau_1)}$	Regimen Factors $[R_I]/[R_{II}]$	Regimen Factors $[R_I']/[R_{II}]$	Correction Factor, $\phi(1-e^{-\omega\tau_1})/\tau_1(1-e^{-\omega\phi})$	Residue Factor, W	Bioavailability Ratio, F_C/F_T
1	1.130	2.566	2.776	1.123	0.126	0.97
2	1.139	2.483	2.700	1.169	0.058	1.05
3	0.914	2.444	2.668	1.190	0.041	0.85
4	1.014	2.219	2.490	1.313	0.006	0.98
5	1.015	2.052	2.366	1.416	0.001	0.98
6	1.732	2.548	2.759	1.133	0.106	1.57
7	0.845	2.190	2.471	1.330	0.004	0.82
8	1.293	2.490	2.706	1.165	0.062	1.19
9	0.750	2.396	2.628	1.216	0.027	0.70
10	1.316	2.499	2.714	1.161	0.067	1.21
11	1.439	2.421	2.649	1.203	0.034	1.37
12	0.810	2.331	2.578	1.251	0.016	0.77

[a] The dose ratio, D_I/D_{II}, used was 1:3.

that $F_C = F_T$. By Eqs. 13 and 14, $[\bar{C}p^{(ss)}]_C$ and F_C/V_0 are projected from $\bar{C}p^{(14,\phi)}$. The time courses of change of plasma levels in accordance with the prescribed dosing sequence are then simulated digitally by the appropriate accumulation of Eq. 15 with due consideration for t_0' and appropriate choices of k_a such that simulated plasma peak times approximate the observed t'_{max}. Finally, the bioavailability ratio of capsule to tablet formulations is calculated from the ratio of $[\bar{C}p^{(7,\tau_1)}]_{sim}$ to $[\bar{C}p^{(7,\tau_1)}]_{obs}$ with the aid of Eq. 16. Individual values of $[\bar{C}p^{(ss)}]_C$, F_C/V_0, k_a, $[\bar{C}p^{(7,\tau_1)}]_{sim}$, and F_C/F_T are summarized in Table III. When comparing corresponding entries in the last column of Table III with those of Table II, it is evident that the two methods of calculation result in similar conclusions.

A comparison of simulated and observed plasma concentrations for a typical subject is shown in Fig. 2. Whereas the perfect agreement between simulated and observed mean plasma levels on Day 14 is predestined as a consequence of Eqs. 13 and 14, their juxtaposition on Day 7 is a function of their relative bioavailabilities. By the same token, the poor agreement point by point is not unexpected, because the method is dependent mainly on area estimates and because the assumptions of a one-compartment open model and of first-order absorption are merely expedients to facilitate the simulation. Nevertheless, the effect of these assumptions on the validity of the conclusion deserves further consideration.

Method C—No attempt is made in the present example to obtain iterative solutions of F_C/F_T by repeated simulations. Instead, a theoretically equivalent calculation is made to illustrate what would have been achieved if such attempts were implemented.

For linear systems, general solutions in closed form descriptive of drug accumulation as a function of time for any tractable dosing sequence were presented previously (7). In the case of a one-compartment open model with first-order absorption, when equal doses are administered at recurring intervals of τ_1, τ_2, and τ_3, the temporal change in plasma concentrations during the ith dosage interval is given by:

$$Cp^{(i)} = \frac{k_a FD}{V_0(k_a-\omega)}\left\{e^{-\omega t}\sum_{\pi,\rho,\sigma}^{i-1} e^{\omega(\pi\tau_1+\rho\tau_2+\sigma\tau_3)} - e^{-k_a t}\sum_{\pi,\rho,\sigma}^{i-1} e^{k_a(\pi\tau_1+\rho\tau_2+\sigma\tau_3)}\right\} \quad \text{(Eq. 19)}$$

where t is real time; and π, ρ, and σ are positive integers such that $(\pi+\rho+\sigma) = 0, 1, 2, \ldots, i-1$, $\pi \geq \rho \geq \sigma$, and $\pi - \sigma \geq 1$.

By applying Eq. 19 specifically to the present example, the mean plasma level following the 19th dose of the tablet formulation can be calculated by specifying $i = 19$ and integrating over the appropriate time intervals:

$$[\bar{C}p^{(7,\tau_1)}]_{sim} = [\bar{C}p^{(i)}]_{sim} \quad \text{(Eq. 20a)}$$

$$[\bar{C}p^{(7,\tau_1)}]_{sim} = \frac{k_a F_T D_T}{\tau_1 V_0(k_a-\omega)}\left\{\frac{[R_a][1-e^{-\omega\tau_1}]e^{-144\omega}}{\omega} - \frac{[R_b](1-e^{-k_a\tau_1})e^{-144k_a}}{k_a}\right\} \quad \text{(Eq. 20b)}$$

where:

$$[R_a] = \sum_{\pi,\rho,\sigma}^{i-1} e^{\omega(\pi\tau_1+\rho\tau_2+\sigma\tau_3)} \quad \text{(Eq. 21)}$$

$$[R_b] = \sum_{\pi,\rho,\sigma}^{i-1} e^{k_a(\pi\tau_1+\rho\tau_2+\sigma\tau_3)} \quad \text{(Eq. 22)}$$

Similarly, the mean plasma level after the seventh dose of the capsule formulation on Day 14 can be calculated by appropriate extensions of Eqs. 19 and 20b:

$$[\bar{C}p^{(14,\phi)}]_{sim} = \frac{k_a F_T D_T}{\phi V_0(k_a-\omega)}\left\{\frac{[R_a'](1-e^{-\omega\phi})e^{-312\omega}}{\omega} - \frac{[R_b'](1-e^{-k_a\phi})e^{-312k_a}}{k_a}\right\} + \frac{k_a F_C D_C}{\phi V_0(k_a-\omega)}\left\{\frac{[R_c](1-e^{-\omega\phi})e^{-312\omega}}{\omega} - \frac{[R_d](1-e^{-k_a\phi})e^{-312k_a}}{k_a}\right\} \quad \text{(Eq. 23)}$$

where:

$$[R_a'] = \sum_{\pi,\rho,\sigma}^{j} e^{\omega(\pi\tau_1+\rho\tau_2+\sigma\tau_3)} \quad \text{(Eq. 24)}$$

$$[R_b'] = \sum_{\pi,\rho,\sigma}^{j} e^{k_a(\pi\tau_1+\rho\tau_2+\sigma\tau_3)} \quad \text{(Eq. 25)}$$

$$[R_c] = (e^{24L\omega})\left(1+\sum_{n=1}^{M-1} e^{n\omega\phi}\right) \quad \text{(Eq. 26)}$$

$$[R_d] = (e^{24Lk_a})\left(1+\sum_{n=1}^{M-1} e^{nk_a\phi}\right) \quad \text{(Eq. 27)}$$

with $j = 21$ and $L = M = 7$.

Table III—Estimates of Bioavailability by Simulations Based on a One-Compartment Open Model

Subject	$[\bar{C}p^{(ss)}]_C$, ng/ml	F_C/V_0, $10^4 \times$ liters^{-1}	k_a, hr^{-1}	$[\bar{C}p^{(7,\tau_1)}]_{sim}$, ng/ml	Bioavailability Ratio, F_C/F_T
1	43.6	1.877	2.40	39.2	1.02
2	74.3	4.333	2.40	68.8	1.05
3	75.3	4.955	0.96	70.9	0.85
4	72.2	7.582	0.36	67.9	0.95
5	52.8	7.316	2.00	53.3	1.03
6	39.5	1.820	0.12	34.7	1.57
7	56.2	6.229	0.84	57.3	0.86
8	68.2	3.896	0.16	63.7	1.22
9	22.4	1.648	0.10	21.4	0.71
10	78.9	4.379	1.00	73.3	1.23
11	54.9	3.819	0.32	52.3	1.38
12	52.0	4.451	2.00	49.0	0.76

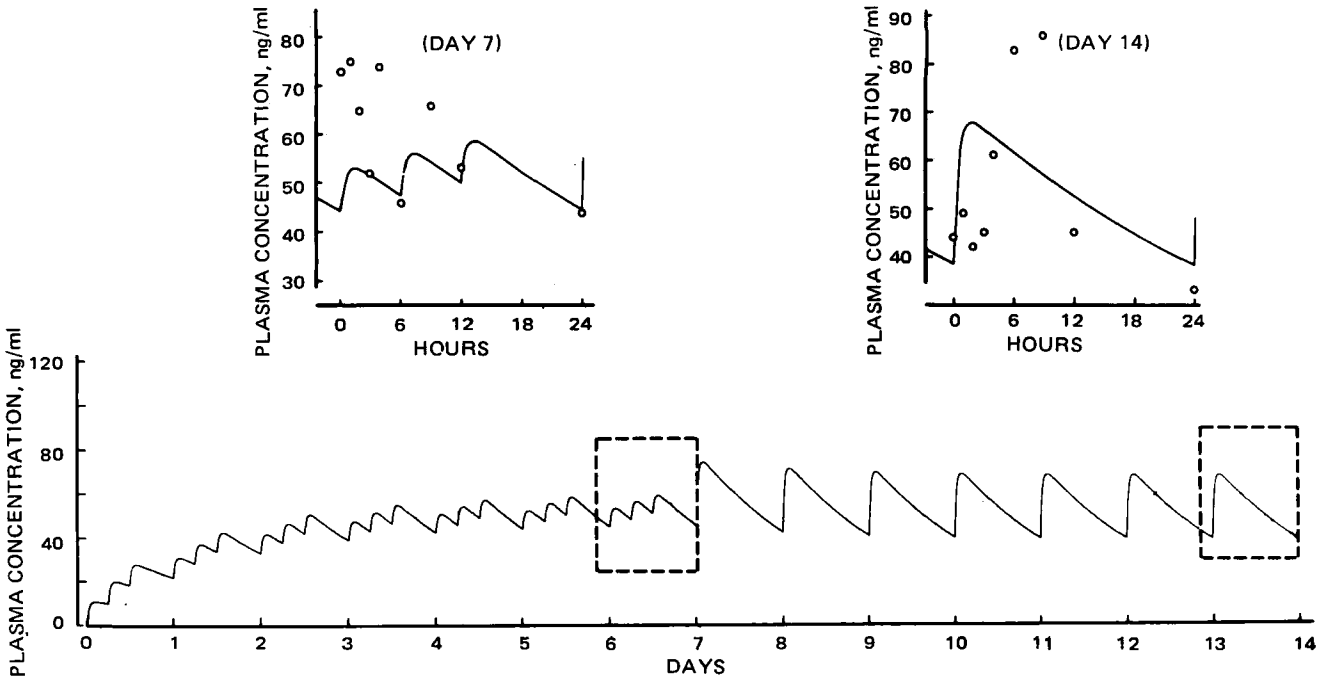

Figure 2—*Typical simulated plasma concentration–time course using a one-compartment open model approximation under the initial assumption of* $F_C = F_T$. *Insets represent enlargements comparing observed (O) and simulated (—) events on Days 7 and 14 (Subject 12).*

The theoretical equivalent of an iterative solution is obtained by replacing the left-hand side of Eqs. 20*b* and 23 by $[\overline{C}p^{(7,\tau_1)}]_{obs}$ and $[\overline{C}p^{(14,\phi)}]_{obs}$, respectively, and solving for F_C/F_T:

$$\frac{F_C}{F_T} = \frac{D_T}{D_C}\frac{[Q_I]}{[Q_{II}]}\left\{\frac{\phi[\overline{C}p^{(14,\phi)}]_{obs}}{\tau_1[\overline{C}p^{(7,\tau_1)}]_{obs}} - \frac{[Q_I']}{[Q_I]}\right\} \quad \text{(Eq. 28)}$$

where:

$$[Q_I] = k_a[R_a]\,(1 - e^{-\omega\tau_1})\,e^{-144\omega} - \omega[R_b]\,(1 - e^{-k_a\tau_1})\,e^{-144k_a} \quad \text{(Eq. 29)}$$

$$[Q_I'] = k_a[R_a']\,(1 - e^{-\omega\phi})\,e^{-312\omega} - \omega[R_b']\,(1 - e^{-k_a\phi})\,e^{-312k_a} \quad \text{(Eq. 30)}$$

$$[Q_{II}] = k_a[R_c]\,(1 - e^{-\omega\phi})\,e^{-312\omega} - \omega[R_d](1 - e^{-k_a\phi})\,e^{-312k_a} \quad \text{(Eq. 31)}$$

There is evidently a close resemblance in form between Eqs. 5 and 28. This finding is not surprising, because the only difference resides in the fact that Eq. 5 is model independent while Eq. 28 is predicated on a one-compartment open model approximation with first-order absorption for the plasma–time course. The application of Eq. 5 requires that the sampled intervals on both Days 7 (τ_1) and 14 (ϕ) begin and end in the log–linear phase. On the other hand, the application of Eq. 28 requires such conformance only on Day 14, so that $[\overline{C}p^{(ss)}]_C$ can be competently estimated from $\overline{C}p^{(14,\phi)}$. In general, only one sampled interval needs to begin and end during the log–linear region, provided an adequate model fits the data adequately in all other sampled intervals. Conversely, when all sampled intervals begin and terminate in ω, Eqs. 5 and 28, and extensions thereof, may be used interchangeably.

The factors $[Q_i]$ in Eq. 28 are composites of terms previously defined (2) as regimen, correction, and residue factors; their identities are readily discernible in Eqs. 29–31. Individual estimates of F_C/F_T by Eq. 28 are shown in Table IV, which also includes values for the factors $[Q_i]$. The values of k_a employed in these calculations were those chosen (Table III) to approximate best the shape of the plasma concentration profiles during τ_1 on Day 7. The agreement between corresponding estimates of F_C/F_T shown in Tables III and IV verifies the previous assertion of equivalence between the two methods of calculation. Figure 3 compares the observed plasma levels and those simulated with the aid of F_C/F_T from Table IV. In contrast to Fig. 2, there is now also equality between simulated and observed mean concentrations during the interval τ_1 on Day 7.

Role of k_a—Estimates of relative bioavailability (Tables III and IV) depend in part on choices of k_a to approximate best the data during τ_1 on Day 7. It is evident from Figs. 2 and 3 that agreement point by point is poor. Thus, an attempt is made to determine the effect of k_a on the estimates of F_C/F_T. It is convenient, and perhaps informative, to classify the results according to the relative magnitudes of k_a to ω (*e.g.*, $\gg 1$, $\simeq 1$, or <1) and to consider each category in relation to previously cited (1) conditions under which the rate of drug accumulation approaches model independence. Table V summarizes the results on selected subjects whose plasma half-lives appear to be representative of the observed range.

When k_a is to be selected from a family, each member of which is much larger than ω, the conditions for model independence are most likely to be satisfied. That is to say, when ω is much smaller than the next larger eigenvalue and when the terminal slope is not k_a, succeeding doses are most probably administered during the log–linear phase. Under these circumstances, the rate of drug accumulation should be predictable from a knowledge of ω. In other words, given an estimate of ω, the observed mean plasma concentration represents a known position in the time course of drug accumulation. Consequently, estimates of F_C/F_T should be relatively insensitive to the choice of a model or parameters therein.

The choice of k_a, even though $>\omega$, becomes progressively more important as the ratio of k_a/ω approaches unity. This result is a manifestation of ω being no longer much smaller than the next larger eigenvalue. The rate of drug accumulation is not entirely predictable from ω alone but is subject also to the residual influence of other eigenvalues. However, a reasonable estimate of F_C/F_T should result, provided the model fits the data adequately during τ_1 on Day 7.

Table IV—Estimates of Bioavailability by Iterations Based on a One-Compartment Open Model (Eq. 28)

Subject	$[Q_I]$	$[Q_I']$	$[Q_{II}]$	$[Q_I]/[Q_{II}]$	$[Q_I']/[Q_{II}]$	F_C/F_T
1	1.530	0.844	2.130	0.718	0.396	0.95
2	1.642	0.423	2.269	0.724	0.186	1.04
3	0.655	0.122	0.908	0.721	0.135	0.83
4	0.232	0.007	0.326	0.712	0.021	0.96
5	1.409	0.008	1.955	0.720	0.004	0.97
6	0.068	0.036	0.095	0.720	0.382	1.53
7	0.576	0.012	0.803	0.717	0.015	0.80
8	0.097	0.030	0.134	0.721	0.223	1.17
9	0.054	0.008	0.075	0.729	0.114	0.69
10	0.668	0.201	0.928	0.720	0.216	1.19
11	0.208	0.034	0.290	0.717	0.116	1.34
12	1.415	0.099	1.951	0.725	0.051	0.77

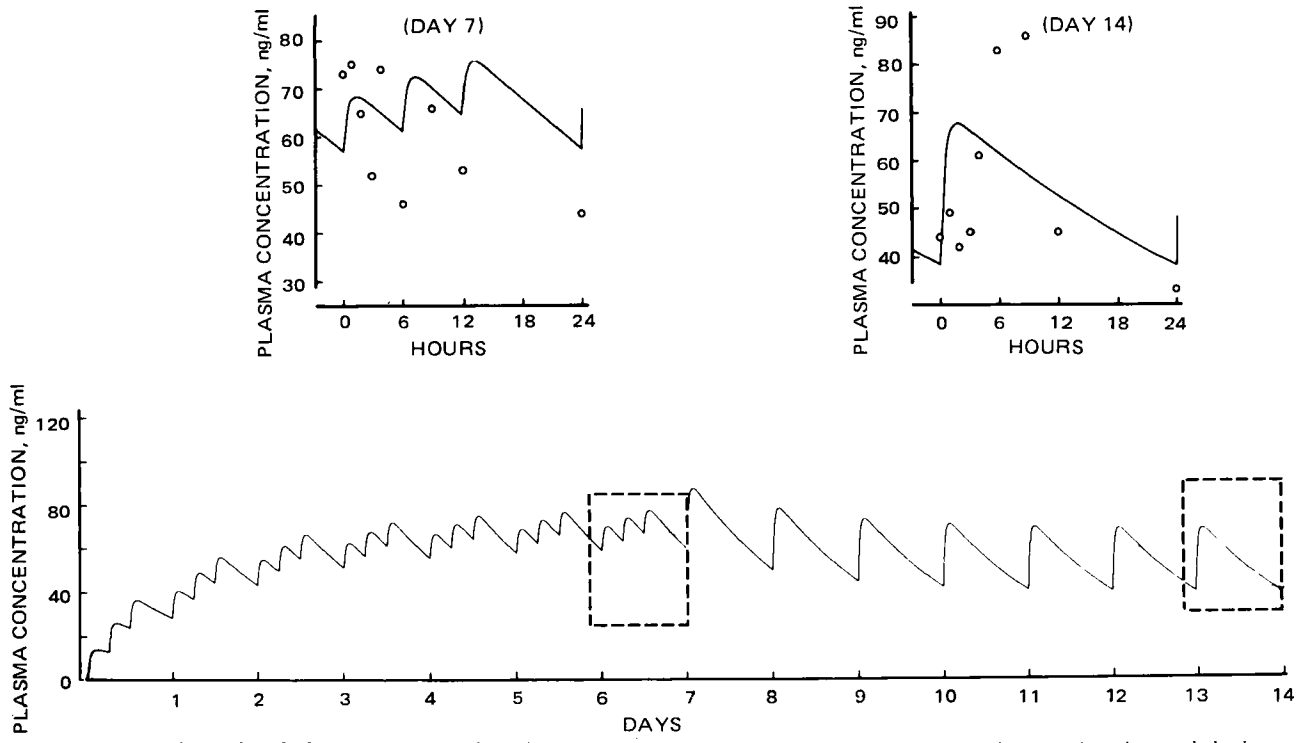

Figure 3—*Typical simulated plasma concentration–time course using a one-compartment open model approximation and the iterative solution of* F_C/F_T. *Insets represent enlargements comparing observed (O) and simulated (—) events on Days 7 and 14 (Subject 12).*

Finally, Table V includes entries for cases where $(k_a/\omega) < 1$, even though the terminology is imprecise. By definition (1), ω is the terminal slope; thus, if k_a is the smallest eigenvalue, it should be properly designated as ω. Nevertheless, this category reflects the magnitude of potential errors resulting from changing half-lives between treatments. If the terminal slope had been experimentally determined for each of the two treatments, one would be designated ω_I and the other ω_{II}, on the basis of which F_C/F_T could be calculated by projections to steady state (2). In the present example, only ω_{II} can be estimated experimentally such that k_a should be viewed simply as the other eigenvalue chosen in an attempt to fit the data on Day 7 by a one-compartment open model. Thus, simulation and iterative techniques may be useful when changes in terminal slope between treatments are suspected but cannot be experimentally verified. They can be attempted if the study design includes at least one sampled interval that begins and ends in the log-linear region.

Table V—Influence of k_a on Estimates of Bioavailability by Eq. 28 for Selected Subjects

	Relative Bioavailability, F_C/F_T				
k_a/ω	Subject 1	Subject 2	Subject 12	Subject 7	Subject 5
0.5	0.18	0.50	0.50	0.67	0.91
0.6	0.28	0.59	0.56	0.72	0.95
0.7	0.36	0.66	0.61	0.75	0.97
0.8	0.43	0.72	0.65	0.77	0.98
0.9	0.49	0.77	0.68	0.79	0.98
1.0	0.54	0.81	0.70	0.80	0.99
2.0	0.80	0.97	0.76	0.82	0.98
3.0	0.87	1.00	0.77	0.81	0.97
4.0	0.90	1.02	0.77	0.81	0.96
5.0	0.91	1.02	0.76	0.80	0.96
6.0	0.92	1.02	0.76	0.80	0.95
8.0	0.93	1.02	0.76	0.80	0.95
10.0	0.93	1.02	0.76	0.79	0.95
12.0	0.93	1.02	0.76	0.80	0.95
14.0	0.93	1.02	0.76	0.80	0.96
16.0	0.93	1.02	0.76	0.80	0.96
18.0	0.94	1.02	0.76	0.80	0.96
20.0	0.94	1.02	0.76	0.80	0.96
Observed (ω, hr^{-1})	0.0133	0.0182	0.0267	0.0347	0.0433

The effect of k_a is negligible for large values of ω but assumes progressively greater significance as ω diminishes, indicating that the model and goodness of fit become less important as steady state is approached.

Model Dependency—An attempt can be made to achieve better agreement point by point on Day 14. The shapes of the plasma concentration profiles suggest that they may be approximated by a two-compartment open model with zero-order absorption.

Slopes, α and β, and apparent intercepts, A' and B', are obtained graphically from the "postabsorptive" phase. The actual intercepts, A and B, at time zero following a single dose can be calculated by correcting for the kinetics during the time of absorption, t_a', and for the influence of all preceding dosages:

$$A = \frac{\alpha t_a' A'(1 - e^{-\alpha\phi})}{(1 - e^{-\alpha t_a'})\{(D_T[R_I']_\alpha W_\alpha/D_C) - [R_{II}]_\alpha\}} \quad \text{(Eq. 32)}$$

$$B = \frac{\beta t_a' B'(1 - e^{-\beta\phi})}{(1 - e^{-\beta t_a'})\{(D_T[R_I']_\beta W_\beta/D_C) - [R_{II}]_\beta\}} \quad \text{(Eq. 33)}$$

from which:

$$\frac{V_1}{F_C} = \frac{D_C}{A + B} \quad \text{(Eq. 34)}$$

The other model parameters, k_{12}, k_{21}, and k_{10}, are calculated in the usual manner. The subscripts α and β on $[R_I']$, $[R_{II}]$, and W signify that ω in Eqs. 7–9 is to be replaced by α or β, as the case may be.

Implicit in Eqs. 32–34 is the assumption that $F_C = F_T$. By analogy, therefore, $[\overline{C}p^{(\tau,\tau_1)}]_{sim}$ can be calculated by appropriate superpositions of Eq. 35, again with due regard for t_0' and t'_{max}:

$$Cp(t) = \frac{k_a' F_T D_T}{V_1}\left\{\frac{(k_a' - k_{21})\, e^{-k_a'(t-t_0')}}{(\alpha - k_a')\,(\beta - k_a')} + \frac{(\alpha - k_{21})\, e^{-\alpha(t-t_0')}}{(k_a' - \alpha)(\beta - \alpha)} + \frac{(\beta - k_{21})\, e^{-\beta(t-t_0')}}{(k_a' - \beta)(\alpha - \beta)}\right\} \quad \text{(Eq. 35)}$$

where k_a' is the fitting constant for apparent absorption which, in general, is different from k_a in Eq. 15 (8). Relative bioavailability between capsule and tablet formulations then can be estimated with the aid of Eq. 16.

Model parameters, including t_a', and estimates of F_C/F_T are shown in Table VI. When comparing the last columns in Tables III, IV, and VI, it is evident that the conclusions are little affected, despite the fact that considerable improvement in point by point agreement has been achieved with the two-compartment open model (Fig. 4). Iterative

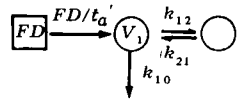

Table VI—Estimates of Bioavailability by Simulations Based on a Two-Compartment Open Model

Subject	Model Parameters[a] from Day 14						$[\bar{C}p^{(\tau,\tau_1)}]_{sim}$, ng/ml	Bioavailability Ratio[a], F_C/F_T
	k_{12}, hr^{-1}	k_{21}, hr^{-1}	k_{10}, hr^{-1}	V_1/F_C, liters	t_a', hr	k_a', hr^{-1}		
1	0.457	0.045	0.204	340	5.0	1.0	41.3	1.08
2	0.620	0.092	0.173	245	4.0	0.6	71.6	1.10
3	0.861	0.124	0.190	217	8.0	0.4	72.6	0.87
4	0.796	0.210	0.182	230	7.0	0.4	72.2	1.01
5	0.505	0.260	0.144	407	6.0	1.0	51.8	1.00
6	0.308	0.106	0.063	1224	5.0	0.2	34.3	1.55
7	0.406	0.118	0.203	279	4.0	0.5	51.1	0.77
8	0.411	0.089	0.121	370	6.0	0.1	62.4	1.19
9	0.619	0.071	0.323	408	7.5	0.1	22.1	0.73
10	1.020	0.079	0.305	125	5.0	0.1	74.0	1.24
11	0.620	0.049	0.507	110	5.0	0.1	51.4	1.35
12	0.264	0.096	0.129	464	6.0	1.0	52.6	0.82

[a] By Eq. 16.

solutions based on simulations of the two-compartment open model are shown in Fig. 5, which is the counterpart of Fig. 3.

There is one important conceptual difference between the one-compartment and the two-compartment simulations attempted in the present example. In the first instance, F_C/V_0 is estimated from $[Cp^{(ss)}]_C$, thus requiring at least one sampled interval to begin and end in the log-linear phase. In the second instance, F_C/V_1 is calculated by modeling the data from a suitable interval and extrapolating to time zero, whereby it is sufficient for the affected interval to terminate in the log-linear phase to provide a starting point to model.

Finally, it is evident that the rate of accumulation varies depending on whether drug disposition is approximated by a one-compartment (Figs. 2 and 3) or two-compartment (Figs. 4 and 5) model. This model dependency is a manifestation of ω being not sufficiently smaller than either E_j or the next larger eigenvalue or both (1). In the present example, since k_a' is always much larger than β (the observed terminal slope), the dependency is attributable to the fact that the term containing $e^{-\alpha\tau_1}$ is not sufficiently close to zero to be ignored or that k_{21} is not always a good approximation of $(k_{21} - \beta)$ or both. Thus, if the two-compartment model is thought to be a more appropriate representation of amitriptyline disposition, the one-compartment model approximation will always underestimate the time course of drug accumulation, particularly during the early stages.

Part of the problem may be overcome by lengthening the sampled interval τ such that $e^{-\alpha\tau} \simeq 0$. However, a better solution, as evidenced by the present example, is to sample at quasisteady state, where model-related differences become negligible.

DISCUSSION

The study comparing amitriptyline formulations was not designed specifically to demonstrate the applicability of the proposed method. Nevertheless, it appears to have been useful in exemplifying the principle of bioavailability assessment at quasi- and nonsteady state and in illustrating some alternative techniques of data analysis. Obviously, there are numerous ways to obtain estimates of bioavailability from a given set of data. Some are theoretical equivalents so that they can be used interchangeably, while others are sufficiently different so that they may be used as checks for each other.

Even though data analysis can be greatly facilitated by keeping

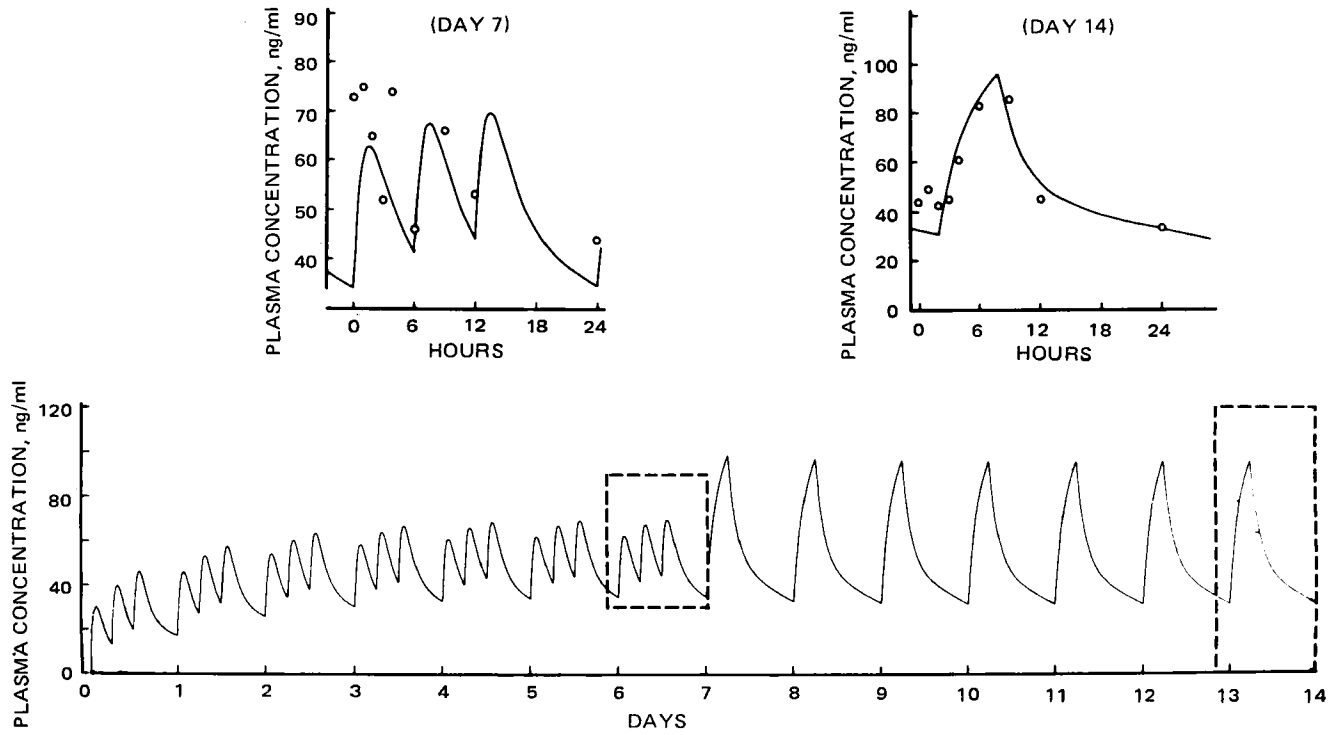

Figure 4—*Typical simulated plasma concentration–time course using a two-compartment open model approximation under the initial assumption of* F_C/F_T. *Insets represent enlargements comparing observed (O) and simulated (—) events on Days 7 and 14 (Subject 12).*

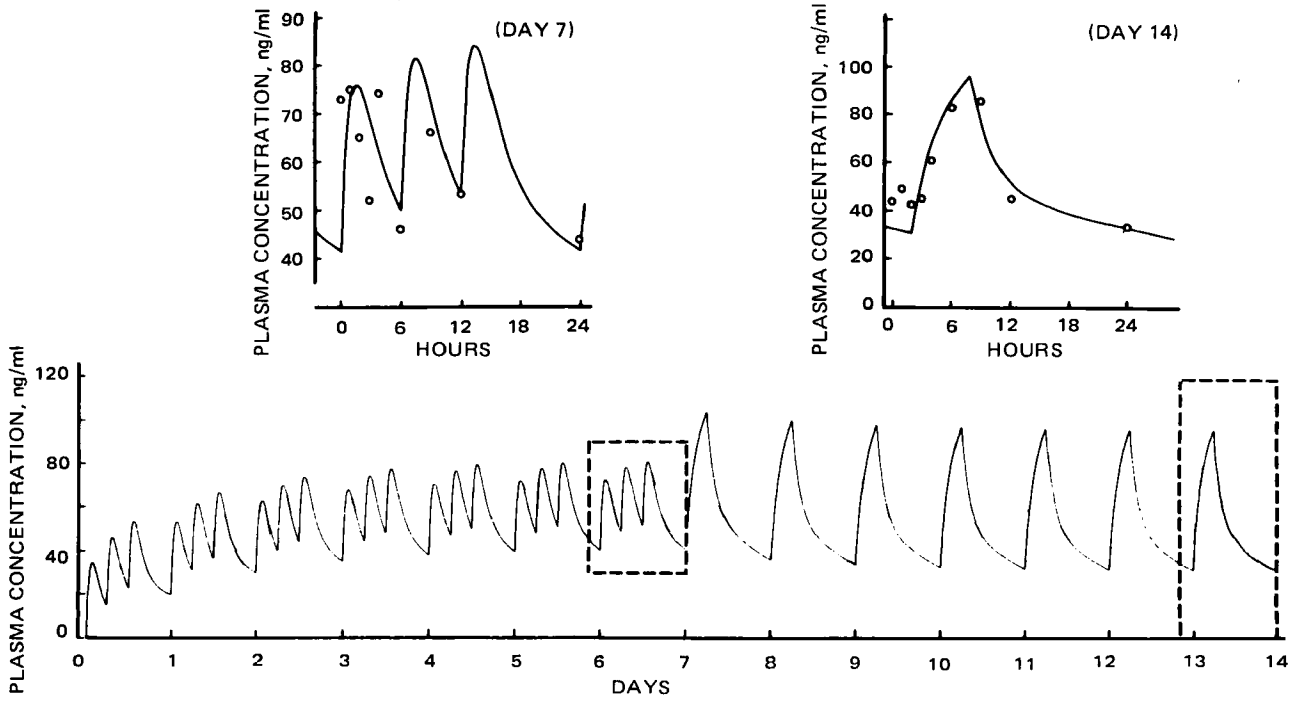

Figure 5—*Typical simulated plasma concentration–time course using a two-compartment open model approximation and the iterative solution of* F_C/F_T. *Insets represent enlargements comparing observed (O) and simulated (—) events on Days 7 and 14 (Subject 12).*

dosages, dosing intervals, and sampling intervals uniform throughout, planned deviations should be considered to accommodate the ease of execution and subject convenience, both of which are particularly important in multiple-dose studies. Analytical options based on extrapolations to steady state require that the sampled intervals begin and end in the log–linear region (2). However, alternatives based on comparative mean plasma levels between simulated and observed values require only that the sample interval over which F/V_0 is estimated begins and ends in the log–linear phase. Finally, if the simulations are predicated on model parameters derived from a suitable dosage interval, it is sufficient that the affected interval terminates in the log–linear region. Thus, the close agreement between corresponding estimates of F_C/F_T in Table II and, for example, Table IV provides verification for one of the underlying assumptions. Namely, the sampled intervals on Days 7 and 14 probably began and terminated in the log–linear phase for most subjects.

In the present example, F/V_0 estimates are derived from data on Day 14, and the temporal changes in plasma concentrations on Day 7 are interpolated through simulation. In general, the sequence may be reversed without compromise with rigor. In other words, it is equally valid to simulate the events on Day 14 through estimates of F/V_0 obtained on Day 7. When all mean plasma levels are determined over intervals beginning and ending in the log–linear region, precise point by point agreement between simulated and observed values is not necessary because an estimate of relative bioavailability would always be possible by projecting the observed means to steady state. This would be true even when ω is identified with k_a, provided that ω is experimentally determined for all affected treatments.

On the other hand, if some sampled intervals begin and terminate under the influence of continued (non-first-order) absorption or before the attainment of pseudosteady state in drug distribution, the validity of the estimated bioavailability ratios would depend on the goodness of fit, the importance of which diminishes as steady state is approached. Therefore, bioavailability assessment at quasi- and nonsteady state may be more or less model independent, depending on drug disposition and experimental design. The relative insensitivity of the present example to alternative methods of calculation is probably the result of having satisfied most of the criteria for model independence; it cannot be generally anticipated.

The techniques employed to effect estimates of bioavailability at quasi- and nonsteady state are simply variations of those used in single-dose and steady-state comparisons. To the extent that a one-to-one correspondence between estimates following single doses and those at steady state can be assured under the principle of superposition, the proposed method is conceptually equivalent to both in that it is a necessary intermediate. Under certain circumstances, there are unique experimental advantages at quasi- and nonsteady state.

In planning single-dose comparisons, sample points must be judiciously placed to ensure a competent estimate of the total area under the plasma–time curve, and sufficient time must elapse between treatments to prevent undesirable residual effects. Whether or not the planned effects are achieved in any given test subject depend largely on the observed terminal slope, which is ascertainable only after the fact. Difficulties may arise when ω is small or when ω cannot be conveniently sampled because it is manifested near or below assay sensitivity or during the subject's normal sleeping hours.

In planning comparisons at steady state, a sufficiently large number of dosing cycles must be included to guarantee experimental attainment of steady state in every treatment; where the dosage and sampled intervals are not uniform throughout, care must be exercised to ensure that all sampled intervals begin and end in the log–linear region. Whether or not the desired effects have been achieved in any given test subject is again dependent on the observed terminal slope and also on subject compliance. Difficulties may arise when so many doses must be given that perfect adherence to the prescribed sequence and timing becomes unrealistic or when the observed ω for some subjects is smaller than anticipated. It is evident that most, possibly all, of these problems can be circumvented at quasi- and nonsteady state. Thus, the proposed techniques appear to be particularly useful when plasma half-lives are long and variable, such as is the case with amitriptyline.

SUMMARY

In summary, some possible techniques for effecting estimates of bioavailability at quasi- and nonsteady state have been illustrated with data from a study comparing two formulations of amitriptyline hydrochloride in humans. It is learned that some previously established (1, 2) experimental constraints may be further relaxed. Minimally, only one sampled interval needs to end in the log–linear region, provided a model can be found to fit the data adequately in all other sampled intervals. There is a demonstrable parallelism in the concepts and in the techniques used to estimate bioavailability, whether the comparisons are made after single doses, at steady state, or somewhere in between.

In a sense, steady-state comparisons can be construed to be a special case of the proposed method in which the residual effect of preceding treatments is zero; and single-dose studies can be considered to be a

special case in which all doses after the first dose of each treatment are skipped to permit more extensive sampling of ω. Conversely, the proposed method may be thought of as a salvage operation for planned steady-state comparisons that fall short of target and for planned single-dose studies where the washout period is too short.

APPENDIX

The validity of Eq. 5 (and, therefore, Eqs. 16 and 28) can be demonstrated with a set of simulated data generated with the aid of a one-compartment open model, in which $F_I = 0.8$, $F_{II} = 0.6$, $k_a = 1.0$ hr^{-1}, $\omega = 0.015$ hr^{-1}, and $V_0 = 10$ liters in accordance with the prescribed regimen. Under these circumstances, the correction factor $\phi(1 - e^{-\omega\tau_1})/\tau_1(1 - e^{-\omega\phi})$ is 1.139; the residue factor W is 0.096; and the regimen factors $R_I = 2.334$, $R_I' = 2.528$, and $R_{II} = 0.920$. Given $D_I = 25$ mg, $D_{II} = 75$ mg, $\bar{C}p^{(I,\tau_1)} = 0.15$ μg/ml, and $\bar{C}p^{(II,\phi)} = 0.13$ μg/ml, $F_{II}/F_I = 0.75$.

REFERENCES

(1) K. C. Kwan, J. V. Bondi, and K. C. Yeh, *J. Pharm. Sci.*, **64**, 1639(1975).

(2) K. C. Yeh and K. C. Kwan, *ibid.*, **65**, 512(1976).

(3) H. B. Hucker, S. C. Stauffer, F. G. Clayton, B. R. S. Nakra, and R. Gaind, *J. Clin. Pharmacol.*, **15**, 168(1975).

(4) H. B. Hucker and S. C. Stauffer, *J. Pharm. Sci.*, **63**, 296(1974).

(5) L. Kirschner, T. H. Simon, and C. E. Rasmussen, *ibid.*, **62**, 117(1973).

(6) P. J. Niebergall, E. T. Sugita, and R. L. Schnaare, *ibid.*, **63**, 100(1974).

(7) K. C. Kwan, M. P. Zirrith, R. A. Castello, and A. D. Marcus, "A Mathematical Treatment of Repetitive Dose Kinetics," presented at the Basic Pharmaceutics Section, APhA Academy of Pharmaceutical Sciences, Dallas meeting, Apr. 1965.

(8) J. C. K. Loo and S. Riegelman, *J. Pharm. Sci.*, **57**, 918 (1968).

ACKNOWLEDGMENTS AND ADDRESSES

Received May 1, 1975, from the *Merck Sharp & Dohme Research Laboratories, West Point, PA 19486*

Accepted for publication January 30, 1976.

[x] To whom inquiries should be directed.

Effect of Formulation of Intramuscular Injections of Phenothiazines on Duration of Activity

A. T. FLORENCE [x], A. W. JENKINS [*], and A. H. LOVELESS

Abstract □ Trifluoperazine and pericyazine were formulated using both the hydrochloride and embonate salts, and some comparisons were made with the activity of fluphenazine salt and ester formulations. Simple solutions in polyethylene glycol, gelled aqueous solutions, nonaqueous suspensions, multiple emulsions, and microencapsulated preparations were formulated, and their duration of activity was tested in dogs. While the multiple emulsion system showed some promise, a nylon microcapsule system produced significant prolonged activity of the drug after deep intramuscular injection.

Keyphrases □ Phenothiazines—effect of various pharmaceutical formulations on duration of biological activity, dogs □ Trifluoperazine hydrochloride and embonate—effect of various pharmaceutical formulations on duration of biological activity, dogs □ Pericyazine embonate—effect of various pharmaceutical formulations on duration of biological activity, dogs □ Pharmaceutical formulations, various—phenothiazines, effect on duration of biological activity, dogs □ Tranquilizers—trifluoperazine hydrochloride and embonate and pericyazine embonate, effect of various pharmaceutical formulations on duration of biological activity, dogs

Long-acting injectable phenothiazines are valuable in extended aftercare therapy in certain psychiatric states (1, 2). Currently available long-acting neuroleptics include solutions in oils such as sesame oil of poorly water-soluble esters of fluphenazine[1] and flupentixol[2], the duration of activity being up to 40 days. However, not all phenothiazines can be esterified to form lipid-soluble derivatives. Therefore, this work was directed toward alternative methods of prolonging the activity of two such drugs, trifluoperazine and pericyazine, using physicochemical rather than chemical or pharmacological methods.

Various formulation techniques, similar to those reviewed by Ritschel (3), were utilized. Resulting preparations were tested in dogs by an apomorphine challenge test utilizing the antiemetic as opposed to the tranquilizing properties of the phenothiazine, since levels of phenothiazine attained cannot be measured readily by available chemical assay techniques. Some experiments were carried out for comparative purposes using fluphenazine embonate. In all cases, fluphenazine enanthate in sesame oil was used as a reference formulation.

EXPERIMENTAL

Materials—Trifluoperazine hydrochloride and embonate salts[3] and pericyazine embonate[3] were used as received. Fluphenazine embonate was recovered after mixing equimolar solutions of sodium embonate[4] and fluphenazine hydrochloride[5]. Fluphenazine enanthate in sesame oil[6] (25 mg/ml) was obtained commercially.

Drug Solubilities—The solubilities of the bases were determined by a turbidity method (4). The solubilized embonate salts were determined by a modification of this method. Various solutions of drug hydrochloride were mixed with buffered sodium embonate (pamoate) to give equimolar mixtures. The turbidity of the solutions at 560 nm was plotted against the final concentration of drug embonate in the

[1] Moditen and Moditen Enanthate, Modecate; Squibb, United Kingdom; Prolixin Enanthate, Squibb, Princeton, N.J.

[2] Depixol, Lundbeck.

[3] May and Baker, Dagenham, Essex, United Kingdom.

[4] Eastman Kodak.

[5] Donated by Squibb, United Kingdom.

[6] Moditen, Squibb.